

THE POLARIZED RAMAN SPECTRA OF
TOURMALINE

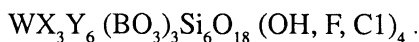
Mingsheng Peng, Ho-kwang Mao,
Liang-chen Chen,
and Edward C. T. Chao*

Polarized Raman spectroscopy (PRS) has been used extensively for structural and compositional characterization of minerals, (White, 1975, Mao *et al.*, 1987, Hemley, 1988). The Raman spectra of minerals are generally analyzed in terms of factor group analysis (McMillan, 1985). For tourmaline with several structural groupings, a general assumption is that its Raman spectra are made of internal modes of each of the individual structural units in the crystal (Si_6O_{18} , BO_3 , OH), plus lattice modes characteristic of the entire unit cell. Each structural unit, $[\text{Si}_6\text{O}_{18}]^{12-}$, $[\text{BO}_3]^{3-}$ and $(\text{OH})^{1-}$, has its distinctive vibrational spectrum.

In this paper we present results of PRS of samples of tourmaline from three different geological occurrences in China, namely granite pegmatites, hydrothermal veins, and metamorphic skarns. Our interest is focussed on the correlation of the PRS to the compositional and structural differences among tourmalines, and the nature of order-disorder of the OH ions in the tourmaline structure in regards to the specific geological occurrences.

*Crystal Structure of Tourmaline and
Description of Samples*

Tourmaline is a complex borosilicate of aluminum varying considerably in composition with a general formula:



where W= Na and Ca; X= Mg, Fe^{2+} , Mn, Al, and Fe^{3+} ; and

Y= Al, Fe^{3+} , Cr, and V.

As shown by Buerger *et al.* (1962), tourmaline has rhombohedral symmetry, and is in the space group $R3m - C_3^v$. The crystal structure is characterized by a layer of six nearly regular SiO_4 tetrahedra in hexagonal arrangement similar to that of a phyllosilicate sheet. The octahedral layer consists of three larger central octahedra containing X cations, six smaller peripheral octahedra containing Y cations, and three boron atoms. The three octahedra of X cations (mainly Mg) shares edges and forms a trigonal unit similar to a brucite $[\text{Mg}(\text{OH})_2]$ -like layer. The trigonal X octahedra unit also share edges with the six Y cations. Each of the boron atoms is in a 3-fold coordination of oxygens at the vertices of octahedra of this layer. The W cation and OH are located along the 3-fold axis of symmetry in the middle of the unit cell. The (OH) hydroxyl groups are confined to three $\text{Mg}(\text{OH})_2\text{O}_4$ octahedra lying in the same layer as the three pairs of $\text{Al}(\text{OH})\text{O}_5$ octahedra.

*U.S. Geological Survey, Mail Stop 929, Reston, VA 22920

TABLE 13. Microprobe analysis of tourmaline of three different types

Types Sample No Color	Pegmatitic		Hydrothermal	Metamorphic	
	TO5 Red	TO4 Lt. Green	TO9 Green	TO6 Blue	TO8 Deep Blue
SiO ₂	37.60	37.05	35.33	34.37	35.1
TiO ₂	0.22	0.50	0.61	0.32	0.21
Al ₂ O ₃	33.30	31.63	33.09	29.83	32.89
FeO	2.19	4.89	4.79	5.43	6.43
MnO	3.30	0.23	0.37	0.18	0.43
MgO	3.65	3.95	8.76	10.05	7.03
CaO	2.37	2.58	0.29	3.36	4.11
K ₂ O	0.11	0.20	0.30	0.64	0.29
Na ₂ O	2.86	2.18	1.66	1.48	1.68
Total	85.6	83.21	85.20	85.66	88.17

The pegmatitic tourmaline samples are from Xinjiang Province in northwest China (samples no. TO5 and TO4). The associated minerals are beryl, columbite, and pollucite. The tourmaline crystals are almost of gem quality. Their color changes from rose-red to green and blue along the *c*-axis. Normal to the *c*-axis, color rings of the same color occurs. The tourmaline from the hydrothermal vein (TO9) came from Hunan province of China. It is associated with quartz and beryl. The tourmaline crystals exhibit prismatic habit. The color ranges from light green to dark green. The tourmalines from metamorphic skarn (TO6 and TO8) came from the tin deposit of Yunnan province of China. The tourmalines have the highest iron content among the three types of samples. The associated minerals are cassiterite, calcite, scapolite and diopside. Chemical compositions of tourmaline samples are listed in Table 13.

Characteristics of PRS of Tourmalines and Assignment of Spectral Peaks

Polarized Raman spectra of tourmaline samples are presented in Table 2. Raman peaks are observed in the regions of 0-1200 cm⁻¹ and 3400-3600 cm⁻¹. Representative spectra are shown in Figs. 64 and 65.

The major peaks of the PRS in the 0-1200 cm⁻¹ region are related to the [Si₆O₁₈]¹²⁻ hexagonal rings (Table 14). Peak assignments are based on the analysis of Raman spectra of a powdered tourmaline sample by Griffith (1969). In the present study, intense Si-O stretching vibration peaks are observed at 1000-1200 cm⁻¹. Two symmetrical ring stretching peaks lie between 400 and 570 cm⁻¹. Two asymmetrical ring stretching peaks lie at 962-999 cm⁻¹ and at 600-700 cm⁻¹. Two ring deformation stretching peaks are located between 220 - 380 cm⁻¹. These two ring deformation stretch-

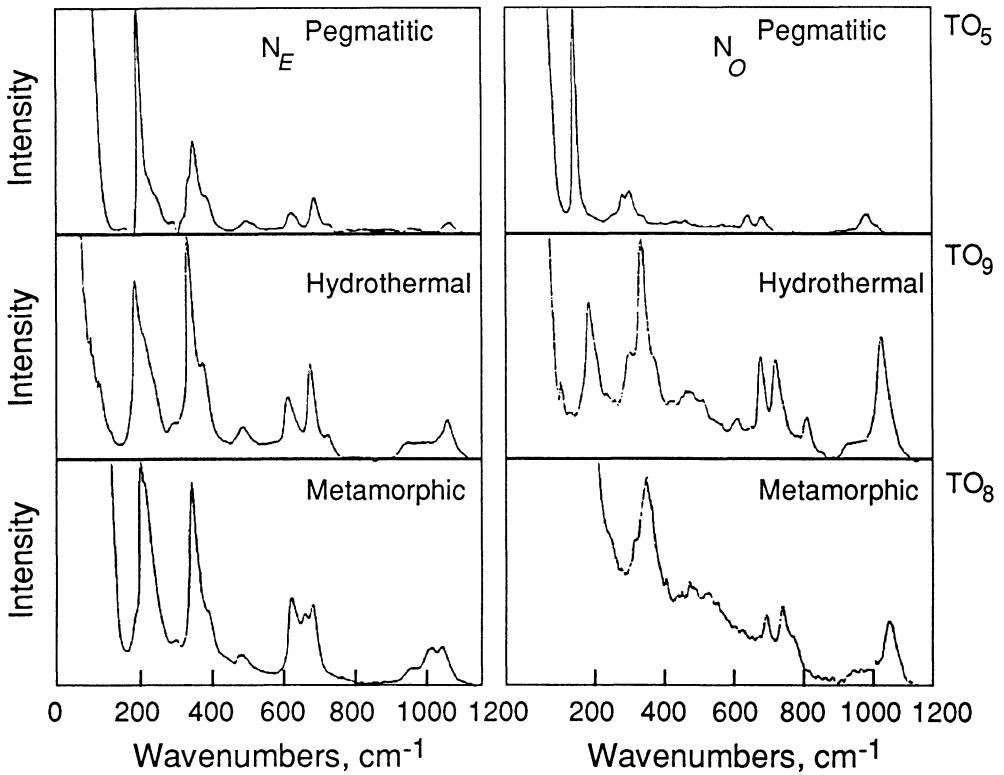


FIG. 64. Polarized Raman spectra of different types of tourmaline in N_E direction and in N_O direction. The ring deformation stretching peaks of $[\text{Si}_6\text{O}_{18}]$ are very strong at 220-380 cm^{-1} . The PRS peak corresponding to the stretching of the B-O bond in BO_3 lies between 700-800 cm^{-1} .

ing peaks are very intense. At different polarization directions, the number of Raman peaks are the same, but the positions of the peaks shift, and the intensities of the peaks vary. The PRS in the N_E direction is much more intense than that of the N_O direction. In addition, as the iron content in the tourmaline increases, the spectral peak splits or distorts, so that the PRS from the granite pegmatite (Fig. 64; TO5) are clearly different from the PRS from the skarn metamorphic tourmaline (Fig. 64; TO8) along the N_O direction.

The PRS peak corresponding to the B-

O bond in $[\text{BO}_3]^{3-}$ lies between 700 and 800 cm^{-1} . Brethous *et al.* (1981) studied Raman spectra of the synthetic system of $\text{B}_2\text{O}_3 - \text{SiO}_2 - \text{Li}_2\text{O}$. By holding the Li_2O content constant but varying B_2O_3 and SiO_2 content, they found that the intensity of the 760 cm^{-1} peak increased with increasing B_2O_3 content, and that the intensity of the peaks at 1040, 950, and 600 cm^{-1} increased with increasing SiO_2 content. Our finding regarding the ring vibrational peaks assigned to Si-O and B-O vibrational peaks is generally consistent with that of Brethous *et al.* (1981). However, the B-O vibration peaks

TABLE 14. Frequencies (cm^{-1}) of polarized Raman spectra of tourmaline in the N_z direction

Types	Pegmatitic		Hydrothermal	Metamorphic		Powdered Samples (Griffith, 1969)
Sample No.	TO5	TO4	TO9	TO6	TO8	
$[\text{Si}_6\text{O}_{18}]^{12-}$				1049	1048	
ν^s (Si-O)	1114	1115	1082(s)	1016(s)	1016(s)	1040(6)
Ring Stretches*	543	540 563	510	527	526	569(5)
	437 404(s)	436 404(s)	403	484	487	464(10)
Ring Stretches**	999 671	998 685	971 638	965 672 633	962 669 634	929(1) 682
Ring deformation	304	342(s)	372(s) 314	363(s) 306	363(s) 306	353(5) 340(1/2)
$[\text{BO}_3]^{3-}$	253(s) 744 734(s)	255(s) 775 737(s)	220(s) 746 703(s)	228(s) 764 693(s)	228(s) 764 692(s)	
$[\text{OH}]^-$						
ν_2	3635	3636	3648	3629	3630	
ν_1	3573(s)	3551(s) 3577	3589(s)	3562(s)	3555(s)	
ν_3	3460	3472	3482	no	no	

* = symmetrical stretching vibration

** = asymmetrical stretching vibration

in tourmaline often split into two peaks. The main splitting is probably due to the variation of bond lengths between boron and adjacent oxygen (B-O₂ bond length is 1.375 Å, B-O₈ bond length is 1.358 Å). The C₃ symmetry of the boron atom is reduced to C_{2v}, and thus the peak splits into two.

Raman peaks in the region between 3400 and 3600 cm⁻¹ are assigned to OH stretching. The peak positions and multiplicities in this region are complicated due to the combined influence of octahedral site occupancies, in- and out-of-phase effects, Al/Si ordering, OH₁/OH₂ ordering, alkali cations (K, Na, Li), and the extent of Al substitution in octahedral and/or tetrahedral sites. The PRS in tourmaline structure peaks assigned to (OH) show clear differences parallel to N_o as compared to N_e. The intensities of the main (OH) band (ν₁) in tourmalines are particularly sensitive to the orientation of the sample.

The blue (Fig. 65; TO6) and deep blue (Fig. 65; TO8) tourmalines from metamorphic skarn have two (OH)¹⁻ stretching vibrational peaks. The most prominent feature in the spectrum of tourmaline is a sharp, intense peak ν₁ at 3550-3590 cm⁻¹ and a weak peak ν₂ at 3630 cm⁻¹. For the blue tourmaline, the two (OH) peaks are located at 3562 (ν₁), and 3629 (ν₂) cm⁻¹. For the deep blue tourmaline, the two (OH) peaks are located at 3555 (ν₁), and 3630 (ν₂) cm⁻¹.

Based on the crystal structure of tourmaline, we know that the (OH) site is at the center of the hexagonal silicon tetrahedra and below the Na ion. The Na-OH bond is 3.285 Å long. The (OH) ion is surrounded by 3 Mg ions which form three octahedra of

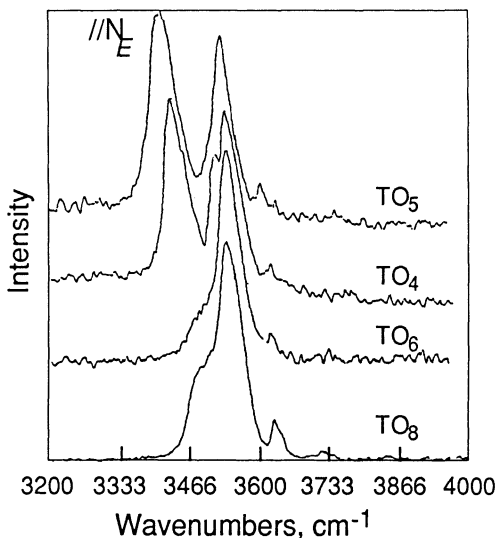


FIG. 65. PRS of [OH]¹⁻ groups in different types of tourmaline in N_e direction at 3400-3650 cm⁻¹. Spectra of tourmalines from metamorphic skarn (TO6 and TO8) and from pegmatite and hydrothermal vein (TO4 and TO5) are plotted.

Mg (OH)₂O₄. The Mg-OH bond length is 2.063 Å. Thus the tourmaline structure contains brucite type (OH) groups.

The vibration peak assigned to (OH) in brucite is shown in Fig. 66 (brucite from U.S. National Museum No. 14390, courtesy of the Division of Mineralogy, U. S. National Museum). A very sharp single peak is observed at 3648 cm⁻¹. The singular peak is due to its high degree of symmetry of (OH) in the brucite structure. The OH group is surrounded by one type of cation (Mg) only. In tourmaline, although the (OH) ion has symmetry similar to that of brucite, the surrounding atoms varies. Thus its symmetry is reduced and the Raman peak splits into two. The deep blue and blue tourmaline of metamorphic skarn origin is high in Fe²⁺ content (Table 13). The Fe²⁺

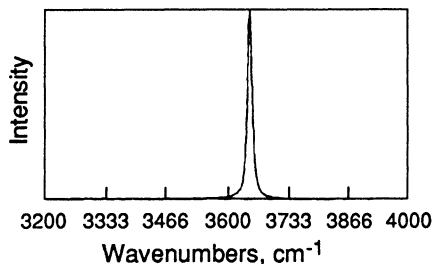


FIG. 66. Raman spectra of brucite $[\text{Mg}(\text{OH})_2]$.

replacement of Mg^{2+} in the $(\text{Mg},\text{Fe})(\text{OH})_2\text{O}_4$ octahedra causes distortion of octahedra and splitting of the OH peak.

The PRS of tourmalines from the granitic pegmatite and from the hydrothermal vein have an additional OH peaks. There are three peaks attributed to (OH) stretching. The rose red Mn-bearing tourmaline has three (OH) peaks at 3460 (ν_3), 3570 (ν_1) and 3635 (ν_2) (Fig. 65; TO5). The three peaks may be accounted for if (OH) occupy two different sites. In addition to the one at the center of the unit all in the middle of the ring as mentioned earlier, (OH) may also substitute an oxygen which surrounds boron atoms, and form an (OHBO_2) ion group. The location of this peak is similar to that of B-O stretching vibrational peak of HOBO_2^- ion (Grice *et al.*, 1986). The light green Fe-bearing tourmaline (Fig. 65; TO4) from the granite pegmatite has 4 peaks where the ν_1 peak splits into two. These four peaks are located at 3472 (ν_3), 3551 and 3577 (ν_1), and 3636 (ν_2).

Conclusion

Based on the PRS of single crystals of

tourmaline, we are able to assign the vibrational spectra to $[\text{Si}_6\text{O}_{18}]^{12-}$, $[\text{BO}_3]^{3-}$, and $[\text{OH}]^{1-}$. The general feature of the polarized Raman spectra (PRS) of tourmaline in the ranges of 200-1200 and 3400-3600 cm^{-1} are presented. Strong peaks of tourmaline were observed at 1000-1200 and 200-400 cm^{-1} . They belong to Si-O stretching vibration and ring deformation vibration of $[\text{Si}_6\text{O}_{18}]^{12-}$. Strong peaks of $[\text{BO}_3]^{3-}$ vibration were measured at 700-800 cm^{-1} . PRS peaks of $[\text{BO}_3]^{3-}$ shift to higher frequencies in the N_o direction.

Strong peak of $(\text{OH})^{1-}$ vibration occurs at 3550-3565 (ν_1) in the N_e direction. The (OH) vibration is strongly polarized. PRS of (OH) can only be detected in the N_e direction. The (OH) group in the metamorphic skarn tourmaline occupies a single site. The site occupancy is ordered. In hydrothermal and granitic pegmatite tourmalines, (OH) occupies two sites with disordered distribution. The (OH) vibrational can be used to characterize site occupancy, and are potentially indicative of the mode of geological occurrences of tourmaline.

References

- Brethous, J. C., A. Levasseur, G. Villeneuve, P. Echegut, and P. Hagenmueller, Studies by spectroscopic Raman and by RMN of the glasses of the system $\text{B}_2\text{O}_3 - \text{SiO}_2 - \text{Li}_2\text{O}$, *J. Solid State Chem.*, 39, 199-208, 1981.
- Buerger, M. H., C. W. Burnham, and D. R. Peacor, Assessment of the several structures proposed for tourmaline, *Acta Crystallogr.*, 15, 583-590, 1962.
- Grice, D. J., and J. V. Velthuisen, Moydite (Y. REE) $[\text{B}(\text{OH})_3(\text{CO}_3)]$, a new mineral species from the evans-lou pegmatite, *Quebec Can.*

- Min.*, 24, 665-673, 1986.
- Griffith, W. P., Raman studies on rock-forming minerals, Part I orthosilicates and cyclosilicates, *J. Chem. Soc. (A)*, 1372-1377, 1969.
- Hemley, R. J., H. K. Mao, and E. C. T. Chao, Raman spectrum of natural and synthetic stishovite, *Phys. Chem. Minerals*, 13, 285-290, 1986.
- Mao, H. K., R. J. Hemley, and E. C. T. Chao, The application of micro-Raman spectroscopy to analysis and identification of minerals in thin section, *Scanning Microscopy*, 1, 495-501, 1987.
- McMillan, P., Vibration spectroscopy in the mineral sciences, *Rev. Mineral.*, 14, Miner. Soc. Am., 9-63, 1985.
- White, B. W., Structural interpretation of lunar and terrestrial minerals by Raman spectroscopy, in *Infrared and Raman Spectroscopy of Lunar and Terrestrial Minerals*, C. Karr, Jr., ed., Academic Press, New York, Chap. 13, pp. 325-356, 1975.

NEW OPTICAL TRANSITIONS IN TYPE IA
DIAMONDS
AT VERY HIGH STRESSES

Russell J. Hemley and Ho-kwang Mao

The generation of ultrahigh pressures in the megabar range is now routine with the diamond-anvil high-pressure cell (Mao, 1988). One of the important features of the diamond-cell arises from the transparency of the diamond anvils to large regions of the electromagnetic spectrum, permitting spectroscopic characterization of materials at high pressures using ultraviolet, visible, and infrared radiation (Hemley *et al.*, 1987). Type Ia diamonds are used in ultrahigh pressure studies owing to the presence of nitrogen platelets which may enhance their strength (Mao *et al.*, 1979). The nitrogen

impurities in these diamonds give rise to a variety of absorption and luminescence systems in the visible and ultraviolet at ambient pressures (Walker, 1979). In optical studies using the diamond-anvil cell, the absorption system at 3 eV in type Ia diamonds serves as an effective absorption edge, precluding most optical measurements at higher energies. Laser excitation in this region gives rise to a broad background fluorescence that can complicate optical measurements of samples within the cell. Further, the enhancement of this luminescence at very high pressure (above 200 GPa) can interfere with measurements of ruby fluorescence used for pressure determination (Mao *et al.*, 1978).

Recently, we performed a series of optical studies of hydrogen and a variety of materials compressed at pressures in the 200 GPa range (Mao and Hemley, 1989; Hemley and Mao, this Report). During the course of this work we discovered dramatic changes in the optical characteristics of the diamonds in the high stress regions (tips) of the anvils. Documenting these effects is essential for further optical studies of materials at pressures above 200 GPa. In particular, this work is a prerequisite for optical characterization of the pressure-induced insulator-metal transition in hydrogen and other systems.

In the present work optical measurements were performed on anvils with 25-50 mm diameter tips, 300-500 mm culets, and bevel angles of 8-10° (see Mao, 1988). As a result of their small tips, at a given load these diamonds generate higher stresses within the anvils than those used in previous spectroscopic studies. The spatial de-